TRENDS IN SCIENCES 2026; 23(2): 11378
https://doi.org/10.48048/tis.2026.11378
RESEARCH ARTICLE

Chemical Profiling and Evaluation of Antibacterial and Anticancer Potential of Endophytic *Aspergillus Terreus* GCD2 Isolated from *Garcinia Cowa* Roxb. ex Choisy: *In Vitro* and *Silico* Approaches

Muhammad Azhari Herli[1,2,4], Putri Ulinza[1], Netti Suharti[5], Djong Hong Tjong[3] and Dian Handayani[1,*]

[1]*Laboratory of Sumatran Biota/Faculty of Pharmacy, Universitas Andalas, Kampus Limau Manis, Padang, Indonesia*
[2]*Department of Biomedical Science, Faculty of Medicine, Universitas Andalas, Padang, Indonesia*
[3]*Department of Biology, Faculty of Mathematics and Natural Sciences, Universitas Andalas, Padang, Indonesia*
[4]*Departement of Pharmacy, Faculty of Mathematics and Natural Sciences, Universitas Muhammadiyah Riau, Riau, Indonesia*
[5]*Department of Microbiology, Faculty of Medicine, Universitas Andalas, Padang, Indonesia*

([*]Corresponding author's e-mail: dianhandayani@phar.unand.ac.id)

Received: 25 July 2025, Revised: 13 August 2025, Accepted: 23 August 2025, Published: 20 November 2025

Abstract

Garcinia cowa Roxb. ex Choisy, a medicinal plant rich in bioactive secondary metabolites, has long been used in traditional medicine for its diverse therapeutic properties. Endophytic fungi associated with medicinal plants have emerged as promising sources of pharmacologically active compounds with antibacterial and anticancer potential in recent years. This study investigates an endophytic fungus isolated from *G. cowa* leaves, identified as *Aspergillus terreus* GCD2 (93.56% BLAST score) through macroscopic, microscopic, and molecular characterization. Crude extracts of GCD2, obtained using ethyl acetate, were profiled via LC-MS/MS, revealing Aurasperone B and Fonsecinone B as the predominant secondary metabolites. Antibacterial activity, evaluated using the Kirby-Bauer diffusion method, showed inhibition against methicillin-resistant *Staphylococcus aureus* (MRSA) with a zone diameter of 12.44 mm. Cytotoxicity testing demonstrated potent bioactivity, with LC_{50} and IC_{50} values of 79.45 µg/mL (Brine Shrimp Lethality Test) and 14.45 µg/mL (MTT assay on MCF-7 breast cancer cells), respectively. Molecular docking simulations indicated strong binding affinities of Aurasperone B and Fonsecinone B to MRSA and breast cancer-related receptors. Against MRSA, both compounds interacted with Asn120 adjacent to the canonical binding site, yielding docking scores of –7.11 and –7.09 kcal/mol (RMSD_refine 0.98 Å and 0.91 Å). Against breast cancer receptors, they bound to Arg146 and Tyr202, with docking scores of –6.00 and –6.20 kcal/mol (RMSD_refine 1.28 Å and 1.32 Å). These findings highlight *A. terreus* GCD2 as a promising source of antibacterial and anticancer agents. Further research focusing on compound isolation, mechanistic studies, and *in vivo* validation is warranted to advance its pharmaceutical potential.

Keywords: *Garcinia cowa* Roxb. ex Choisy, *Aspergillus terreus*, Endophytic fungi, Antibacterial, Cytotoxicity, Molecular docking, Aurasperone B, Fonsecinone B

Introduction

Garcinia cowa Roxb. ex Choisy, locally known as asam kandis, is a medium-sized evergreen tree naturally distributed across several Asian countries, including Nepal, East India (Assam, Bengal, Bihar, Mizoram, and Orissa), Cambodia, Laos, Malaysia, Myanmar, Thailand, Vietnam, and Indonesia. This plant's distinctive morphological and phytochemical characteristics contribute to its extensive use in traditional medicine. Phytochemical analyses have revealed that *G. cowa* contains diverse bioactive

compounds, including despidones, flavonoids, phenolglucinols, terpenes, steroids, and xanthones [1-3].

Scientific investigations have confirmed the medicinal potential of *G. cowa*, attributing its therapeutic effects to its richness in secondary metabolites such as flavonoids, terpenoids, phenolics, and steroidal compounds. With the increasing demand for safer and more sustainable therapeutic agents, plant-derived natural products are gaining recognition as promising alternatives to synthetic drugs. However, their integration into modern therapeutic applications requires rigorous scientific validation to ensure efficacy, safety, and sustainability. Comprehensive toxicological, pharmacological, and conservation studies are essential to regulate and optimize their medicinal use. *G. cowa* has been reported to exhibit a broad spectrum of biological activities, including antimicrobial, anti-inflammatory, antioxidant, antimutagenic, antiplatelet, anticancer, and antidiabetic effects. Compared to synthetic agents, plant-based extracts often offer advantages regarding biocompatibility and environmental safety. Consequently, the bioactive secondary metabolites of *G. cowa* continue to attract considerable interest in natural product research, particularly for their potential applications in drug discovery and ethnopharmacology [4-7].

In recent years, there has been a notable shift from relying solely on medicinal plants to exploring microorganisms, particularly microbes and microbiomes, as alternative and promising sources of secondary metabolites. This paradigm shift has fueled interest in endophytic fungi-microorganisms that inhabit the internal tissues of plants without causing apparent harm to their hosts. Endophytic fungi have garnered significant attention due to their ability to synthesize a broad spectrum of bioactive compounds with potential applications in medicine, agriculture, and biotechnology. These symbiotic organisms contribute to plant health by promoting growth, enhancing resistance to biotic and abiotic stress, and producing metabolites that may mimic or surpass those of their host plants. Notably, endophytic fungi are prolific producers of structurally diverse and pharmacologically significant secondary metabolites, such as anthraquinones, sesquiterpenoids, and cyclic peptides, many of which exhibit potent antibacterial, antifungal, and anticancer activities [8,9]. Their metabolic versatility makes them a valuable resource for drug discovery and developing novel therapeutic agents. Accordingly, investigating endophytic fungi from medicinal plants offers a sustainable and environmentally friendly route to identifying novel metabolites with therapeutic potential.

Endophytic fungi isolated from *G. cowa* have demonstrated promising antibacterial activity, particularly against common and drug-resistant bacterial strains. These microorganisms produce a wide array of bioactive secondary metabolites capable of inhibiting bacterial growth. A previous study successfully isolated 13 endophytic fungal strains from *G. cowa*, among which the GCA3 isolate, identified *as Penicillium citrinum*, exhibited notable antibacterial activity, with inhibition zones of 15.05 ± 0.51 mm against *Staphylococcus aureus*, 14.68 ± 0.50 mm against *Escherichia coli*, and 13.48 ± 0.15 mm against methicillin-resistant *Staphylococcus aureus* (MRSA) [10]. The antibacterial properties of these endophytes are primarily attributed to their ability to synthesize potent antimicrobial metabolites, which are influenced by the host plant species and their growth media—an important factor in addressing the global challenge of multidrug-resistant pathogens [9]. In addition to antibacterial activity, bioactive compounds from endophytic fungi associated with *G. cowa* have shown anticancer potential. However, these compounds remain insufficiently characterized. This aligns with broader findings that endophytic fungi can produce structurally diverse molecules with efficacy against various bacterial species and cancer cell lines [11].

Despite the reported bioactivities of *G. cowa*-associated endophytes, there is still limited research on the comprehensive characterization of their bioactive metabolites, particularly those with dual antibacterial and anticancer potential. Moreover, studies integrating chemical profiling, biological evaluation, and molecular docking to elucidate possible mechanisms of action remain scarce. The present study investigates an endophytic fungus isolated from *G. cowa* leaves, identified as *Aspergillus terreus* GCD2, to address this gap. The study aims to (i) characterize its secondary metabolites using LC-MS/MS, (ii) evaluate its antibacterial activity against MRSA, (iii) assess its cytotoxic effects through Brine Shrimp Lethality Test (BSLT) and [3-(4,5-Dimethylthiazol-2-yl)-2,5-Diphenyltetrazolium Bromide] (MTT) assays, and (iv)

explore molecular interactions of its key metabolites with antibacterial and anticancer target proteins through docking simulations. The findings are expected to contribute to discovering novel bioactive compounds from endophytic fungi and support their potential development as sustainable therapeutic agents.

Materials and methods

Sample materials

The materials used in this study consisted of 13 ethyl acetate extracts of endophytic fungi isolated from *G. cowa* Roxb. ex Choisy (asam kandis) plants, obtained from previous studies [10].

Methods

Brine shrimp lethality test (BSLT)

The Brine Shrimp Lethality Test (BSLT) is a widely used preliminary bioassay for evaluating the general toxicity of natural product extracts and screening for bioactive compounds. *Artemia salina* L. (family: Artemiidae) nauplii were used in this assay. Brine shrimp eggs were incubated in 500 mL of filtered seawater under continuous aeration for 48 h at 27 ± 2 °C to allow hatching. Post-hatching, active nauplii were collected and distributed into experimental vials. Each test group contained ten nauplii exposed to varying concentrations of the GCD2 fungal extract (1,000, 500, 100, 50, and 10 µg/mL) dissolved in dimethyl sulfoxide (DMSO). The negative control group received only DMSO in sterile seawater. After 24 h of incubation at room temperature, mortality was recorded, and the median lethal concentration (LC_{50}) was calculated using probit analysis based on the mortality data [12,13].

Cell culture and MTT cytotoxicity assay

The MTT assay was performed to evaluate the cytotoxic effects of the ethyl acetate fraction of the GCD2 fungal extract on MCF-7 human breast cancer cells, following the procedure described by Kumar *et al.* [14] and Meerloo *et al.* [15]. MCF-7 cells were obtained from the Cancer Chemoprevention Research Center (CCRC), Faculty of Pharmacy, Gadjah Mada University, and cultured in Dulbecco's Modified Eagle Medium (DMEM) supplemented with 10% fetal bovine serum (FBS) and 1% penicillin–streptomycin. Cells were seeded in 96-well plates at a density of 6×10^3 cells/well in 100 µL of medium and incubated overnight at 37 °C in a humidified atmosphere containing 5% CO_2.

A stock solution of the fungal extract was prepared in dimethyl sulfoxide (DMSO) at 100,000 ppm. After 24 h, the culture medium was removed, and cells were washed with sterile phosphate-buffered saline (PBS). Subsequently, 100 µL of treatment solution (100 ppm extract in medium) was added to each well. The experimental design included treatment groups, a positive control (Paclitaxel), a cell control (untreated cells), and a media control (blank). Following treatment, plates were incubated for 24 h under the same conditions. Cell viability was determined by adding MTT solution, incubating, and measuring absorbance at 540 nm using an ELISA microplate reader. The absorbance values were used to calculate the percentage of viable cells, measuring the extract's cytotoxicity [14,15]. % Cell viability is calculated by the equation [15,16].

$$\frac{\text{OD of treatment} - \text{OD of blank}}{\text{OD of control} - \text{OD of blank}} \times 100\%$$

Determination of IC_{50} value

The cytotoxicity of the fungal extracts was further quantified by determining the half-maximal inhibitory concentration (IC_{50}) using the same MTT assay protocol described for sample screening. The ethyl acetate extract of the GCD2 fungus was tested at concentrations of 500, 250, 125, 62.5 and 31.25 ppm. Paclitaxel was the positive control and tested at concentrations of 100, 50, 10, and 5 ppm. The IC_{50} value was calculated from the dose–response curve by plotting the percentage of cell viability against the logarithmic concentration of the sample. The resulting curve was analyzed to determine the concentration at which cell viability was reduced by 50% [15,16].

Statistical methods

To determine the IC_{50} values, the natural logarithm of the sample concentrations (ln [concentration]) was regressed against the corresponding percentage of cell viability. The resulting regression equation was used to estimate the IC_{50}, defined as the concentration at which cell viability was reduced by 50%. Alternatively, IC_{50} values were also calculated using probit analysis with

statistical software (SPSS) to provide more precise interpolation [15,16].

LC-MS/MS analysis of endophytic fungi extracts GCD2

The bioactive extract of GCD2 fungi that showed good antibacterial and cytotoxic activity was then analysed using a Liquid Chromatography-Mass Spectrometry (LC-MS/MS) instrument with UPLCQToF-MS/MS (Ultra Performance Liquid Chromatography-Quadrupole Time of Flight-Mass Spectrometry) specifications to determine the compounds contained. Liquid chromatography-tandem mass spectrometry is an analytical technique that combines liquid chromatography as a component separator in a sample with mass spectrometry as a detector. This study used a tandem mass spectrometry-based tool, MassLynx version 4.1 [17]. MassLynx version 4.1 is the default software for the Water LC-MS/MS tool, a widely used software for processing and interpreting mass spectrometry data to identify phytochemicals. It can read raw data from the water LCMS/MS results in MS1 and MS2, which are then searched for compound annotation in an online database. Compound annotation utilised online databases such as MassBank (https://massbank.eu/MassBank/), the Human Metabolome Database (HMDB, https://www.hmdb.ca/), and ChemSpider (https://www.chemspider.com/), with ion fragmentation pattern matching used to distinguish compounds with similar m/z values. The ionisation process was conducted at 2 energy levels: Low energy (4 V) to detect precursor ions and high energy (25 - 60 V) to obtain fragment (daughter) ions. When searching for compounds by molecular formula, a hydrogen atom (1.00782 Da) was subtracted to account for protonation during ionisation, resulting in a positively charged molecular ion [18-20].

Morphology and molecular identification of endophytic fungi

The morphological identification of the purified endophytic fungal isolate was initially conducted based on macroscopic and microscopic characteristics. Macroscopic features such as colony color, texture, margin, and growth rate were observed on Sabouraud Dextrose Agar (SDA) after incubation at room temperature (25 °C) for 5 - 7 days. Microscopic examination was performed by preparing slide cultures stained with lactophenol cotton blue and observing the hyphal structure, conidiophores, vesicles, and spore morphology under a light microscope. Genomic DNA was extracted for molecular identification, and the internal transcribed spacer (ITS) region of ribosomal RNA was amplified using universal fungal primers. The ITS region comprises 4 parts: The large subunit rRNA, ITS1, 5.8S rRNA, and ITS2. The amplification and sequencing procedures followed the methodology described by Sandrawati *et al.* [11]. This work was conducted collaboratively between Genetica Science Indonesia (Tangerang, Banten) and the Environmental Biotechnology Laboratory (EBL) of the Indonesian Center for Biodiversity and Biotechnology (ICBB), Bogor, West Java, reflecting a joint commitment to robust and accurate species identification.

PCR products were sequenced by First BASE Laboratories (Malaysia), using high-throughput sequencing technology to ensure data quality and reliability. The resulting sequences were analyzed using the BLAST tool (https://blast.ncbi.nlm.nih.gov/Blast.cgi) to compare with sequences in the NCBI GenBank database. Species identification was performed based on the closest sequence similarity, following the approach described by Tallei and Kolondam. [21]. A phylogenetic tree was constructed using the neighbor-joining method with 1,000 bootstrap replications to confirm taxonomic placement. MEGA software (https://www.megasoftware.net/dload_win_beta) [22] was used to generate the tree and evaluate genetic relationships among related fungal species. The fungal isolate GCD2 was identified as *Aspergillus terreus* based on morphological features and ITS sequence homology.

Molecular docking analysis

The bioactive compounds identified through LC-MS/MS analysis were evaluated using molecular docking simulations with the Molecular Operating Environment (MOE) 2024.06 software. The MRSA receptor and breast cancer receptor were selected from the RCSB Protein Data Bank (https://www.rcsb.org/). MOE was used for docking simulations to determine how well the compounds could bind to the active site's MRSA receptor (PDB ID: 6Q9N) and breast cancer receptor (PDB ID: 6O0K) [23-26]. The basis for conducting molecular docking simulations on MRSA

receptors is the inhibitory power of ethyl acetate extract from the endophytic fungus GCD2, as reported in previous research on MRSA, which was 12.44 mm [10]. Meanwhile, docking simulations using breast cancer receptors are based on examination results using BSLT (shown in **Table 1**) and MTT Test data IC_{50} in this research (IC_{50} value of the ethyl acetate extract of the endophytic fungi *A. terreus* (GCD2) is 14.45 μg/mL).

Molecular docking simulation begins with preparing the target protein, followed by preparing test ligands and native ligands. The docking process involves the interaction of test ligands and native ligands with the receptor's active site. The final stage consists of validating the molecular docking process and interpreting the results [27]. The target receptor was prepared in MOE using a quick preparation method, which aims to optimise the receptor structure by correcting the protonation and optimising the receptor's charge. Ligand testing in the preparation seeks to optimise the ligand energy with the MMFF94X force field, correcting the ligand charge and ligand structure to obtain an optimal ligand structure ready for molecular docking simulations. In the docking procedure, a range of binding modes was generated, and the one with the least binding energy, emphasising kcal/mol, was chosen as the most optimal [28]. Visualisation of ligand binding with receptors in 2D and 3D molecular docking results using BIOVIA Discovery Studio Visualizer software (https://discover.3ds.com/discovery-studio-visualizer-download) [29].

Results and discussion

Medicinal plants have long been recognized for their health benefits and have been widely used in traditional medicine for centuries. Today, they are often utilized in the form of extracts, valued for their therapeutic efficacy and relatively low side effects. However, the limited production of secondary metabolites in native medicinal plants can restrict access to their bioactive compounds. Over time, the overharvesting of these plants can also lead to the gradual depletion of their natural resources. Endophytes, which include bacteria, fungi, algae, and actinobacteria, are microorganisms that live inside plants without causing visible symptoms. They have been detected in all plant species, suggesting an ancient and co-evolved relationship between plants and their endophytes. This association is mutually beneficial: the host plant provides nutrients and shelter, while the endophytes enhance the host's resilience against biotic and abiotic stresses. Among endophytes, fungi are fascinating due to their ability to produce diverse bioactive molecules, often mirroring those their host plants synthesize. This biochemical similarity suggests that endophytic fungi can serve as alternative and sustainable sources of pharmacologically active secondary metabolites. Numerous studies have reported that endophytic fungi isolated from medicinal plants can produce compounds with therapeutic properties equivalent to those of their hosts, offering potential in drug discovery and natural product development [8,30-32].

The findings of this study reinforce the view that endophytic fungi are a promising alternative source for discovering new therapeutic agents. This work forms part of an ongoing effort to identify bioactive compounds from endophytic fungi isolated from diverse sources, including marine sponges, mangrove trees, and medicinal plants from West Sumatra, Indonesia [10,11,33,34]. Extensive research has also examined the chemical composition and biological activities of various parts of *G. cowa* Roxb. ex Choisy. Previous investigations on its fresh leaves, fruits, and dried bark have revealed that the main constituents are organic acids and their lactones, which contribute significantly to its pharmacological properties [3,5,6].

Screening of antibacterial activity, based on the results of previous studies [10], and cytotoxicity of endophytic fungal extracts derived from *G. cowa* Roxb. ex Choisy (asam kandis) were evaluated using the agar diffusion method and the Brine Shrimp Lethality Test (BSLT), respectively. The results are summarized in **Table 1**.

Table 1 Antibacterial activity and toxicity screening (BSLT) of endophytic fungal extracts from *G. cowa* Roxb. ex Choisy.

Fungal code	Organ	Average of inhibition zone (mm)			LC50 (ppm)
		S. aureus	MRSA	*E. coli*	
GCA1	Root	11.23	10.09	10.35	128.41
GCA2	Root	11.9	11.67	11.13	89.09
GCA3	Root	14.11	15.4	15.22	370.06
GCB1	Stem	10.37	11.25	9.5	190.12
GCB2	Stem	9.91	12.1	10.06	97.47
GCB3	Stem	7.42	8.93	7.73	147.59
GCB4	Stem	11.6	12.95	12.2	257.8
GCD1	Leaf	-	-	-	4.87
GCD2	Leaf	22.72	12.44	11.521	79.45
GCD3	Leaf	11.43	11.04	7.39	191.43
GCD4	Leaf	-	-	-	319.06
GCD5	Leaf	8.09	8.73	8.13	83.19
GCD6	Leaf	8.55	8.68	8.64	89.29
Positive Control	-	30.22	30.19	30.59	-

Positive control: Oxoid® disks containing 30 µg/mL chloramphenicol

Among the thirteen extracts tested, several exhibited notable antibacterial activity accompanied by varying degrees of cytotoxicity, as indicated by their LC_{50} values. The ethyl acetate extract GCD2 demonstrated the broadest antibacterial spectrum, significantly inhibiting *S. aureus* (22.72 ± 0.01 mm), *E. coli* (11.521 ± 0.002 mm), and MRSA (12.44 ± 0.02 mm). It also showed appreciable cytotoxicity, with an LC_{50} value of 79.45 µg/mL, suggesting its potential as a bioactive candidate for pharmaceutical development. In contrast, extract GCD1 displayed the lowest LC_{50} value, indicating higher cytotoxicity, but lacked measurable antibacterial activity.

Based on these results, GCD2 was selected for further investigation, including cytotoxicity testing against MCF-7 breast cancer cells, chemical profiling using LC-MS/MS, and molecular docking analysis of its active compounds with antibacterial and anticancer target proteins. Overall, extracts GCA3, GCD1, and GCD2 emerged as promising candidates due to their antibacterial efficacy and acceptable cytotoxicity profiles. Notably, GCD2's selective potency, including activity against resistant Gram-negative bacteria, highlights its potential as a valuable source for developing novel antibacterial agents.

Molecular identification and morphology of endophytic fungi GCD2

The endophytic fungus GCD2, isolated from the leaf of the asam kandis plant (*G. cowa* Roxb. ex Choisy), was identified using macroscopic and microscopic examinations. On Sabouraud Dextrose Agar (SDA) medium, GCD2 colonies appeared cream to brown, often with clumps exhibiting yellow pigmentation. Microscopic observation using a Binocular TCLG microscope revealed distinctive morphological features

compared with standard fungal identification keys and literature. GCD2 displayed compact, columnar conidial heads measuring up to 500 µm in length with a diameter of 30 - 50 µm [35,36]. The conidiophores bore hyaline, smooth-walled, spherical conidia with diameters of 1.5 - 2.5 µm (**Figure 1**). Molecular identification was conducted by sequencing the internal transcribed spacer (ITS) region, a widely recognized molecular barcode for fungi due to its high interspecific variability and strong discriminatory power at both genus and species levels. BLAST analysis revealed a 93.56% sequence similarity to *Aspergillus terreus*, confirming the taxonomic identity of GCD2 (**Figure 2**).

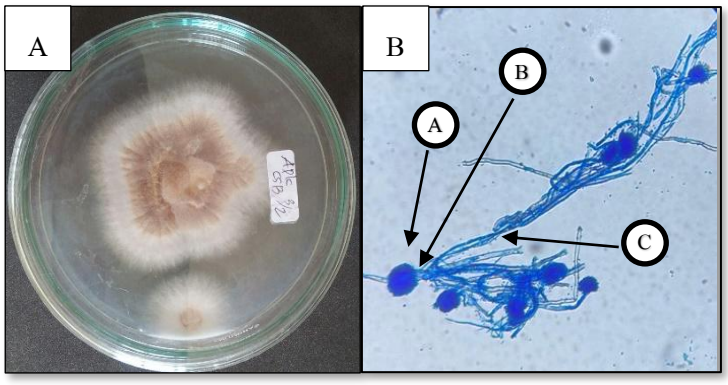

Note: a. Conidia, b. Fialid, c. Conidiophores

Figure 1 Macroscopic (A) and microscopic (B) pictures of fungal isolate GCD2.

Forward 2303.02079 (GCD2)

GTGACCGGCAGAGCTCAAATTTGAAATCTGGCTCCTTCGGGGTCCGCATTGTAATTTGCAGAGGATGCTTCGG
GTGCGGCCCCCGCCTAAGTGCCCTGGAACGGGCCGTCAGAGAGGGTGAGAATCCCGTCTGGGGCGGGGTGT
CTGCCCCCGTGTAAAGCTCCTTCGACGAGTCGAGTTGTTTGGGAATGCCCCTCTAAATGGGTGGTAAATTTCAT
CTAAAGCTAAATACTGGCCGGAGACCGATAGCGCACAACCGCAGTGATCGAATGATGAAAAGCACTTTGAAA
AAATAGTTAAACGCCACGTGAAATTGTTGAAAGGGAAGCGCTTGCAACCAGACCCGCTCGCGGGGTTCAGCC
GGCCTTCCCTCCGGTGTACTTCCCCGCGGGCGGGCCTGCGTCGGTTTGGGCGGCCGGTCAAAGGCCCCCGGA

Result 2303.02079: (GCD2)

Aspergillus terreus strain F12 large subunit ribosomal RNA gene, partial sequence. Homology 93,56%
Query Cover 100%

Figure 2 DNA sequence at the ITS region of the endophytic fungi isolated from the asam kandis (*G. cowa* Roxb. ex Choisy) Plant was aligned by the MEGA software.

Phylogenetic analysis based on ITS region sequences

A phylogenetic analysis was performed using the neighbor-joining method in MEGA software, based on ITS region sequences and comparison with the NCBI database (https://blast.ncbi.nlm.nih.gov/Blast.cgi). The phylogenetic tree was constructed to determine the genetic relationship between the endophytic fungus GCD2 (*Aspergillus terreus*) and other related endophytic fungal species [37]. As shown in **Figure 3**, GCD2 clusters closely with *A. terreus* and *Aspergillus* sp., indicating a closer genetic relationship with these species than with *A. neoindicus* or *A. carneus*.

Figure 3 Phylogenetic Tree of endophytic fungi GCD2.

Toxicity and cytotoxicity test

BSLT and MTT assay

The Brine Shrimp Lethality Test (BSLT) results showed that the LC_{50} values of the ethyl acetate extracts from the fungal isolates ranged from 1 to 335 ppm. According to Lestari *et al.* [38], plant or animal extracts are classified as cytotoxic if the LC_{50} value is < 1,000 ppm. Specifically, extracts with LC_{50} < 30 ppm are considered highly toxic, 30 - 1,000 ppm are considered toxic, and > 1,000 ppm are considered non-toxic. For pure compounds, an LC_{50}< 200 ppm is regarded as toxic. Based on this classification, the ethyl acetate extract of endophytic fungus GCD2, with an LC_{50} of 79.45 µg/mL, falls within the toxic category and warrants further investigation for potential anticancer compounds.

The BSLT has been reported to correlate reasonably well with cytotoxic activity against certain human solid tumors and has contributed to the discovery of promising new classes of antitumor agents. The LC_{50} value of 79.45 µg/mL obtained for GCD2 indicates toxicity to the test organism (*Artemia salina* larvae), suggesting the potential for toxic effects in humans, particularly at high doses. However, determining its safety for human use will require further toxicity evaluations, including both *in vitro* and *in vivo* studies in appropriate animal models, followed by clinical assessments. Cytotoxic agents can disrupt fundamental cellular processes, including growth, mitosis, differentiation, and function. The observed cytotoxic activity of the ethyl acetate extract in this study may be attributed to one or more of these mechanisms. Further cytotoxicity evaluation was performed using the microtetrazolium (MTT) assay against MCF-7 human breast cancer cells, obtained from the CCRC Laboratory, Faculty of Pharmacy, Universitas Gadjah Mada. This colorimetric assay measures cell viability based on mitochondrial enzyme activity and allows determination of the half-maximal inhibitory concentration (IC_{50}), defined as the concentration of the extract or compound that inhibits 50% of cell viability [14,15].

The extract was tested at concentrations of 500, 250, 125, 62.5 and 31.25 µg/mL, each in triplicate. Initial screening indicated that the ethyl acetate extract of GCD2 produced the lowest cell viability (≤ 50%) against MCF-7 cells at a concentration of 31.25 µg/mL. IC_{50} determination was subsequently performed on this extract using linear regression analysis of the dose–response curve, yielding an IC_{50} value of 14.45 µg/mL. For comparison, the positive control, Paclitaxel,

exhibited an IC_{50} of 11.09 µg/mL. According to the National Cancer Institute (NCI) and the classification by Niksic *et al.* [39], compounds with $IC_{50} \leq 20$ µg/mL are considered highly cytotoxic, 21 - 200 µg/mL moderately cytotoxic, 201 - 500 µg/mL weakly cytotoxic, and > 500 µg/mL inactive. Based on these criteria, the ethyl acetate extract of *A. terreus* (GCD2) demonstrates highly cytotoxic activity against MCF-7 cells, positioning it near the threshold of this category.

In this preliminary study, we report a significant finding: the secondary metabolites present in the fungal extract exhibit potent cytotoxic activity. This result is highly valuable, as it provides a strong basis for future research aimed at isolating and structurally characterizing cytotoxic compounds from the endophytic fungus *A. terreus* GCD2. The demonstrated potential of this extract as a source of novel drug candidates for cancer treatment highlights its importance and underscores the relevance of continuing investigations into its bioactive constituents.

Identification of secondary metabolite content

The fungal extract of GCD2 was analyzed using Liquid Chromatography-Tandem Mass Spectrometry (LC-MS/MS) equipped with an Ultra-Performance Liquid Chromatography–Quadrupole Time-of-Flight Mass Spectrometer (UPLC-QToF-MS/MS). This high-resolution analytical technique was employed to identify bioactive secondary metabolites potentially responsible for the extract's cytotoxic activity. The sensitivity and mass accuracy of UPLC-QToF-MS/MS enable precise detection and structural characterization of various compound classes, including phenolics, flavonoids, alkaloids, and terpenoids, many of which are associated with anticancer properties [11,18].

Mass spectrometry data were acquired and processed using MassLynx™ software, which generated chromatograms and MS spectra for molecular weight determination and formula prediction. Compound identification was achieved by matching the observed molecular formulas and fragmentation patterns with those available in public MS databases, including MassBank, the Human Metabolome Database (HMDB), and ChemSpider. To ensure accurate compound annotation, MS/MS spectra were compared with reference fragmentation data, accounting that isobaric compounds may share similar m/z values but differ in fragmentation behavior. The MS system was operated in dual-energy mode: low collision energy (4 V) was used to detect intact parent ions ($[M + H]^+$), while high collision energy (25 - 60 V) was applied to generate daughter ions for structural elucidation. Protonation during electrospray ionization was considered by subtracting 1.00782 Da from the [M + H]+ ion, ensuring accurate molecular mass calculations [19,20].

LC-MS/MS analysis of the ethyl acetate extract from the endophytic fungus *A. terreus* GCD2 generated a chromatogram with several prominent peaks at distinct retention times (**Figure 4**). These data were used to identify secondary metabolites present in the extract. Six bioactive compounds were detected, representing naphthopyran, benzophenone, chromone, cyclic peptide, and phenol groups (**Table 2**). Among these, Aurasperone A exhibited the highest peak intensity in the chromatogram, indicating it as the major constituent. Aurasperone A, a dimeric naphthopyran, has been previously reported to possess various biological activities, including cytotoxic and antimicrobial properties [40,41]. Its abundance in the extract suggests a possible contribution to the observed cytotoxic activity against MCF-7 breast cancer cells, although further mechanistic investigations are required to confirm this role.

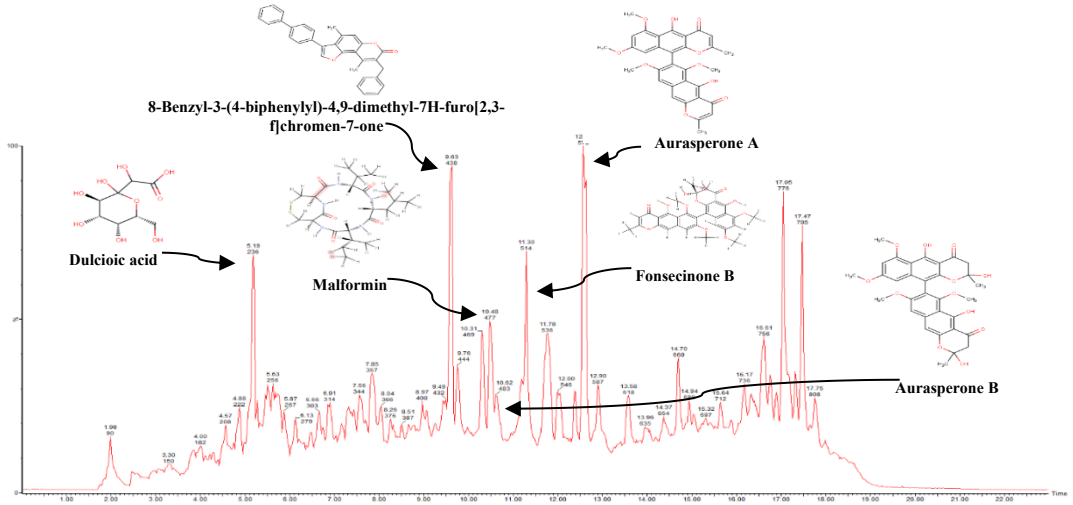

Figure 4 LC-MS/MS chromatogram of the ethyl acetate extract from the endophytic fungus *A. terreus* GCD2.

Table 3 Chemical composition of the ethyl acetate extract from the endophytic fungus *A. terreus* GCD2, identified by LC-MS/MS in positive ion mode, including compound names, chemical classes, retention times, and peak intensities.

Compound's name	Molecular formula	Mass	RT (mins)	Parent on (m/z)
Dulcioic acid [42]	$C_7H_{12}O_8$	224.165 g/mol	5.19	224.0566
8-Benzyl-3-(4-biphenylyl)-4,9-dimethyl-7H-furo[2,3-f]chromen-7-one [43]	$C_{32}H_{24}O_3$	456.541 g/mol	9.63	457.1761
Malformin [44]	$C_{23}H_{39}N_5O_5S_2$	529.7 g/mol	10.46	530.249
Aurasperone B [45]	$C_{32}H_{30}O_{12}$	606.6 g/mol	10.63	607.1821
Fonsecinone B [46]	$C_{32}H_{28}O_{11}$	588.6 g/mol	11.30	589.1708
Aurasperone A [47]	$C_{32}H_{26}O_{10}$	570.550 g/mol	12.57	571.1611

Molecular docking simulation

To explore its therapeutic relevance, molecular docking simulations were performed to assess the binding affinity and interaction profiles of six bioactive compounds with two types of target proteins, as shown in **Tables 4** and **5**. The first molecular docking simulation to determine the interaction between the ligand structure and the MRSA receptor, using the crystal structure of PBP2a MRSA (PDB ID: 6Q9N), which is part of the mecA gene, was performed with a resolution of 2.50 Å. This structure consists of 2 main chains, namely chain A and chain B, with a sequence length of 642 amino acids. This structure has 3 ligands: QLN, JPP, and MUR. The active binding site is on chain A at the XYZ centre coordinates –17.749267; –25.286833; 69.861767 with a radius of 10.034159 [25,26].

In the second molecular docking simulation to determine the interaction between the ligand structure and the breast cancer (BCL-2) receptor, the crystal structure of BCL-2 (PDB ID: 6O0K), which is involved in the apoptosis of cancer cells, was utilized, with a resolution of 1.62 Å. This structure consists of a single main chain, designated as chain A, with a sequence length of 166 amino acids. This structure has 2 ligands: LBM and 2PE. The active binding site is on chain A at the XYZ centre coordinates –15.323057; 2.213738; –9.593467 with a radius of 13.647127 [23,24].

As shown in **Table 4**, the native ligand of the MRSA receptor showed a binding score of –6.84 kcal/mol. In comparison, Aurasperone B and

Fonsecinone B showed slightly lower scores of –7.11 kcal/mol and –7.09 kcal/mol, respectively, but Aurasperon A showed a slightly higher score of –5.67 kcal/mol. Aurasperone B (–7.11 kcal/mol) and Fonsecinone B (–7.09 kcal/mol) also showed slightly lower scores compared to the antibacterial drugs quinazolinone (–6.83 kcal/mol) and piperacillin (–6.95 kcal/mol) (**Table 4**). However, Aurasperone B and Fonsecinone B exhibit a more complex interaction pattern, featuring additional van der Waals and carbon-hydrogen interactions (**Figure 5**). For the bonding interaction between Aurasperone B and Fonsecinone B, when compared with the native ligand, there is the same bonding interaction with the amino acid residues at TYR 79, ILE 118, GLU 119, for hydrophobic interactions, as well as the amino acid residue ASN 120 specifically for hydrogen bonding interactions in Aurasperone B. Furthermore, Aurasperone B and Fonsecinone B exhibited a lower RMSD_refine value (0.98 Å and 0.91 Å) compared to the redocking native ligand (1.92 Å, **Figure 5(D)**), Quinazolinone (1.66 Å), and piperacillin (1.54 Å) (antibacterial drugs as control), suggesting a more stable docking pose with less deviation during refinement [48,49].

Table 4 Results of molecular docking simulations and Interactions with residue amino acid residues of MRSA Receptors (PDB ID: 6Q9N).

Protein Target	Ligand	S Value (kcal/mol)	RMSD refine (Å)	Interaction	
				Hydrogen Interaction	Hydrophobic Interaction
6Q9N	Dulcic acid	–4.71	1.31	-	ASN 71, SER 72, TYR 105, ILE 144, GLU 145, ASN 146, ASN 204, TYR 297, SER 306, ASN 307, THR 308
	8-Benzyl-3-(4-biphenylyl)-4,9-dimethyl-7H-furo[2,3-f]chromen-7-one	–5.46	1.67	-	ASN 71, SER 72, TYR 105, ILE 144, ASN 146, LYS 273, GLU 294,ASP 295, TYR 297, ASN 305, SER 306, ASN 307, THR 308, LYS 316
	Aurasperone B	–7.11	0.98	ASN 120, LYS 247	ASN 78, TYR 79, ILE 118, GLU 119, ASP 248, ASP 249, ASP 269, TYR 271, LYS 290, ASN 923
	Malformin	–6.45	1.68	CYS 2, TYR 79	-
	Fonsecinone B	–7.09	0.91	LYS 247, ASP 249, LYS 290	TYR 79, ILE 118, GLU 119, ASN 120, ASP 249, GLU 268, ASP 269, TYR 271
	Aurasperone A	–5.67	1.95	-	SER 72, ASN 104, TYR 105, ASN 146, ASN 204, TRP 205, GLY 296, ASP 303, SER 306, ASN 307, THR 308, ILE 309
	Native_Ligand 6Q9N	–6.84	1.92	ASN 120	TYR 79, ILE 118, GLU 119, THR 184, PHE 185, ASN 923, THR 924, ILE 925

Protein Target	Ligand	S Value (kcal/mol)	RMSD refine (Å)	Interaction	
				Hydrogen Interaction	Hydrophobic Interaction
	Quinazolinone	–6.83	1.66	ASN 120, THR 916	TYR 79, ILE 118, GLU 119, HIS 759, GLU 761, VAL 918, ASN 923, THR 924, ILE 925
	Piperacillin	–6.95	1.54	SER 46, ASN 78, TYR 79	ASN 78, ASN 120, TYR 271

*Residues in bold and underlined indicate the active site residues of the target protein.

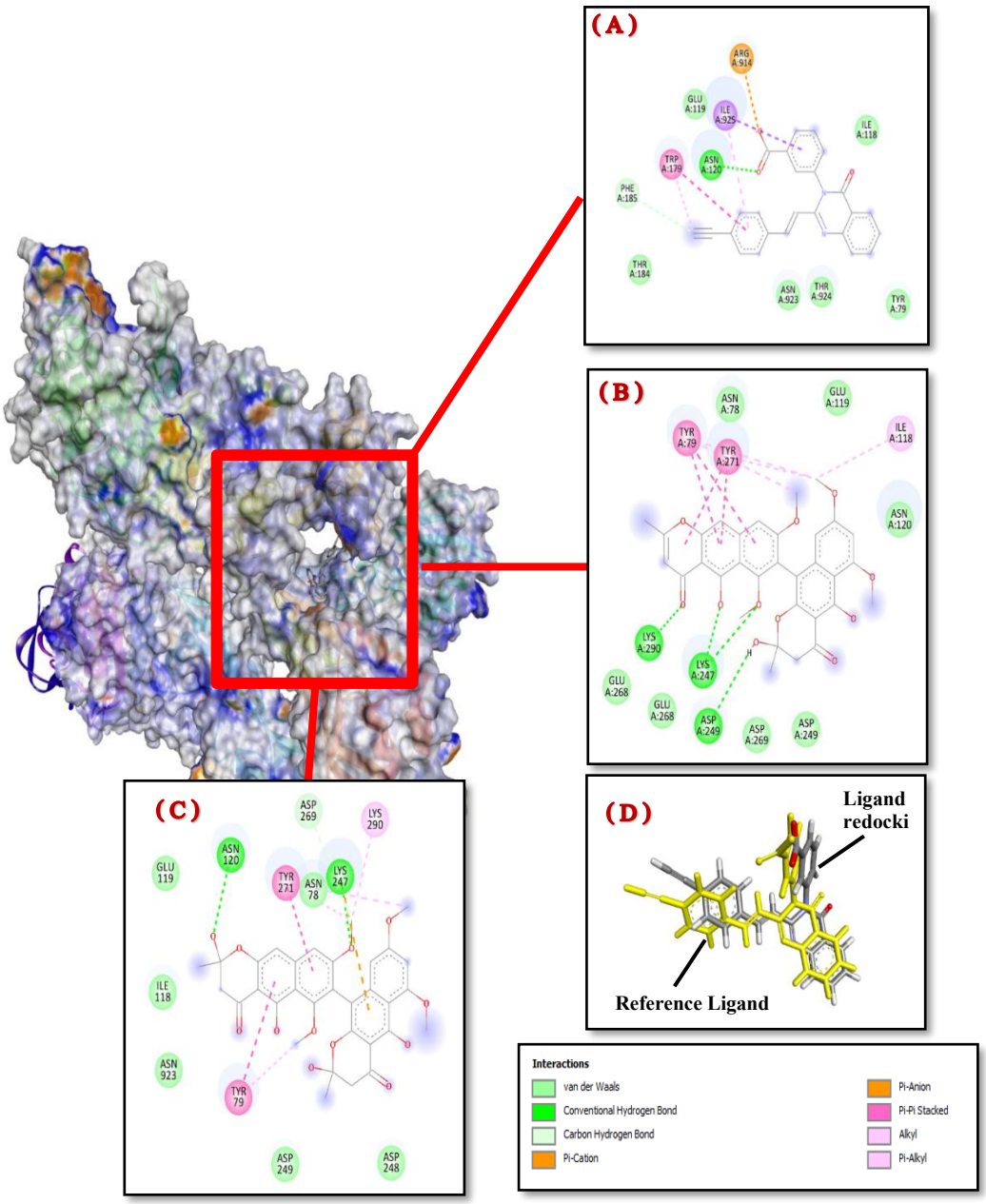

Figure 5 Molecular interaction of the best compounds and antibacterial drugs with essential amino acid residues of the MRSA Receptor (PDB ID : 6Q9N). (A) Native Ligand (B) Fonsecinone B, (C) Aurasperone B, and (D) Redocking Native_ligand (RMSD: 1.92 Å).

In **Table 5**, the native ligand of the BCL-2 receptor shows a binding score of –11.40 kcal/mol. Aurasperone A, Aurasperone B, and Fonsecinone B show higher scores, respectively, –6.20 and –6.00 kcal/mol (**Table 5**). When compared with obatoxlac, which is an Anti-cancer drug with a binding score of –5.17 kcal/mol, the binding values of Aurasperone A, Aurasperone B, Fonsecinone B, and 8-Benzyl-3-(4-biphenylyl)-4,9-dimethyl-7H-furo[2,3-f]chromen-7-one are slightly lower and richer in Van der Waals bonds, hydrogen bonds, and π bonds.

For the bonding interaction of Fonsecinone B compared with the native ligand, there is the same bonding interaction with the amino acid residues at ALA 100, ARG 107, TYR 108, ARG 146, ALA 149, for hydrophobic interactions, as well as the amino acid residue TYR 202 specifically for hydrogen bonding interactions in Fonsecinone B. Furthermore, Aurasperone A, Aurasperone B, Fonsecinone B, and 8-Benzyl-3-(4-biphenylyl)-4,9-dimethyl-7H-furo[2,3-f]chromen-7-one exhibited a lower RMSD_refine value (2.10 Å, 1.28 Å, 1.32 Å, and 1.64 Å) compared to the native ligand and obatoclax (2.14 Å and 2.12 Å), suggesting a more stable docking pose [48].

Table 5 Results of Molecular Docking Simulations and Interactions with residue Amino Acid Residues of Breast Cancer receptors (PDB ID: 6O0K).

Protein target	Ligand	S Value (kcal/mol)	RMSD refine (Å)	Interaction	
				Hydrogen interaction	Hydrofobic interaction
6O0K	Dulcioic acid	–4.67	2.29	-	PHE 104, ASP 111, MET 115, VAL 133, LEU 137, ASN 143, GLY 145, ALA 149
	8-Benzyl-3-(4-biphenylyl)-4,9-dimethyl-7H-furo[2,3-f]chromen-7-one	–6.40	1.64	-	GLN 99, PHE 104, ARG 106, ARG 107, TYR 108, LEU 137, GLY 145, ALA 149, PHE 198
	Aurasperone B	–6.00	1.28	ARG 146	PHE 104, SER 105, TYR 108, ASP 111, PHE 112, MET 115, VAL 133, GLU 136, LEU 137, ARG 139, ASP 140, ALA 149, PHE 153, VAL 156
	Malformin	–5.84	1.82	ARG 146	PHE 104, TYR 108, ASP 111, MET 115, GLN 118, VAL 133, GLU 136, LEU 137, ASP 140, GLY 145, ALA 149, PHE 153

Protein target	Ligand	S Value (kcal/mol)	RMSD refine (Å)	Interaction	
				Hydrogen interaction	Hydrofobic interaction
	Fonsecinone B	–6.20	1.32	TYR 202	GLN 99, ALA 100, ASP 103, PHE 104, ARG 107, TYR 108, ASN 143, TRP 144, GLY 145, ARG 146, VAL 148, ALA 149, PHE 198
	Aurasperone A	–6.49	2.10	ARG 146	SER 105, TYR 108, ASP 111, VAL 133, GLU 136, ASP 140, GLU 152, PHE 153
	Native_Ligand 6O0K	–11.40	2.14	ASN 143, TRP144, GLY 145, TYR 202	ALA 100, ARG 107, TYR 108, ASP 111, PHE 112, MET 115, LEU 137, ARG 146, ALA 149, VAL 156
	Venetoclax	–8.30	1.91	GLY 145, ARG 146	ALA 100, ASP 103, PHE 104, TYR 108, ASP 111, PHE 112, MET 115, VAL 133, GLU 136, LEU 137, ASN 143, TRP 144, VAL 148, ALA 149, PHE 153, PHE 198, TYR 202
	Navitoclax	–8.57	2.32	TYR 108, ARG 146	GLN 99, ALA 100, ASP 103, PHE 104, ARG 106, ARG 107, ASP 111, GLU 114, MET 115, GLN 118, GLU 136, LEU 137, ASP 140, ASN 143, GLY 145, VAL 148, TYR 202
	Obatoclax	–5.17	2.12	-	THR 96, GLN 99, ALA 100, ASP 103, ARG 107, ASN 143,

Protein target	Ligand	S Value (kcal/mol)	RMSD refine (Å)	Interaction	
				Hydrogen interaction	Hydrofobic interaction
					TRP 144, GLY 145, VAL 148, TYR 202, GLY 203
	Paclitaxel	–7.33	1.35	-	ALA 100, PHE 104, TYR 108, ASP 111, PHE 112, MET 115, VAL 133, GLU 136, ASN 143, GLY 145, ARG 146, VAL 148, ALA 149, PHE 153, PHE 198, TYR 202
	Doxorubicin	–7.22	1.31	ASP 103	THR 96, GLN 99, ALA 100, PHE 104, ARG 107, TYR 108, TRP 144, GLY 145, VAL 148, TYR 202, GLY 203

*Residues in bold and underlined indicate the active site residues of the target protein.

The validity of the molecular docking process was assessed by calculating the root mean square deviation (RMSD) of the redocked native ligand relative to its initial (reference) position within the target protein. An RMSD value ≤ 2 Å is generally considered acceptable, indicating that the docked ligand's position closely matches its original orientation [27,50,51]. In the 1st molecular docking simulation with the MRSA receptor, the RMSD for the redocked native ligand was 1.92 Å (**Figure 5(D)**). In the 2nd simulation with the BCL-2 receptor, the RMSD was 2.14 Å (**Figure 6(E)**). Both results fall within the acceptable threshold, confirming the reliability of the docking protocol.

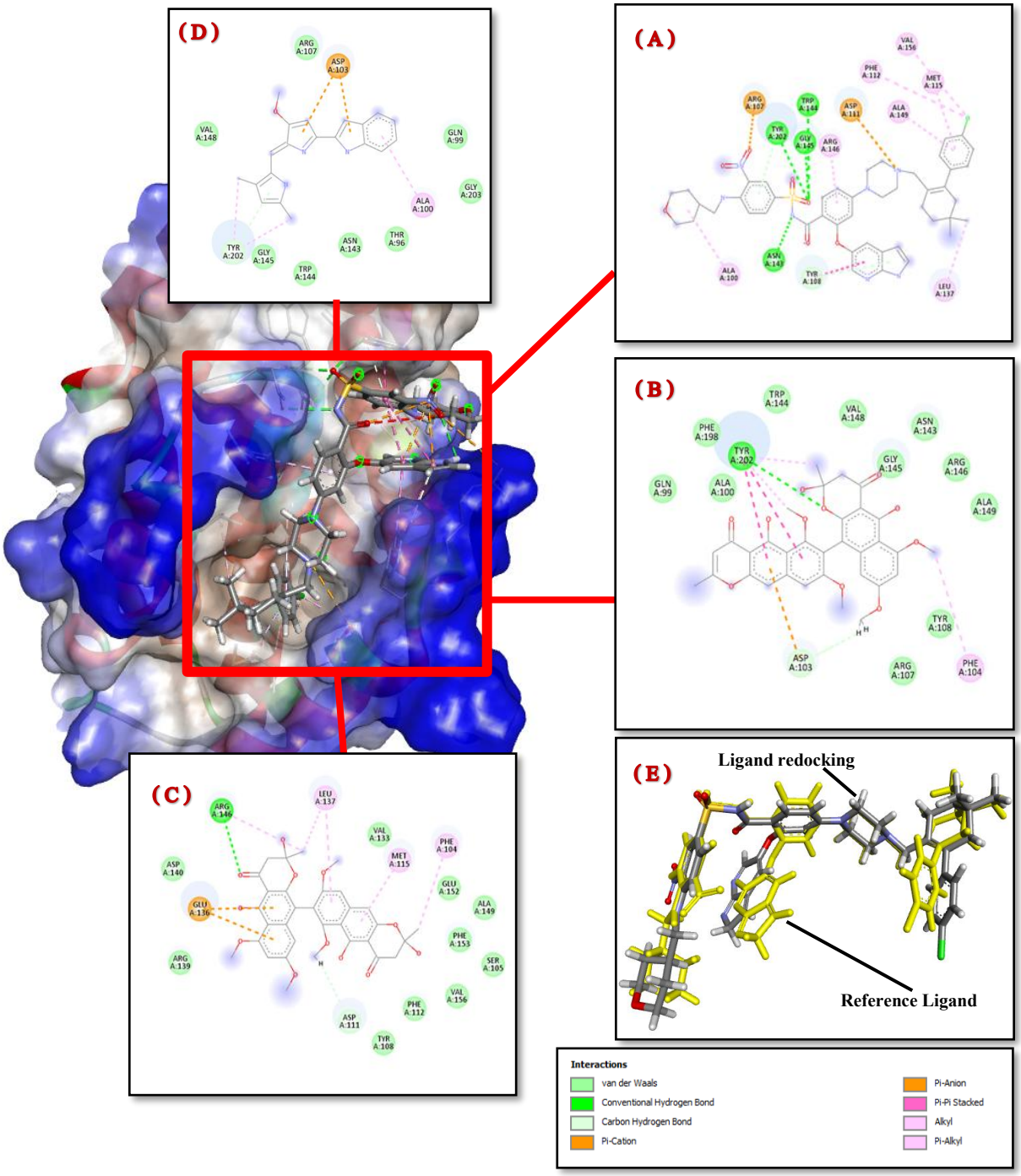

Figure 6 Molecular interaction of the best compounds with essential amino acid residues of BCL-2 Receptor (PDB ID: 6o0k). ((A) Native Ligand, (B) Fonsecinone B, (C) Aurasperone B, (D) Obatoclax, and (E) Redocking Native_ligand (RMSD: 2.14 Å).

Conclusions

LC-MS/MS profiling of the endophytic fungus *A. terreus* GCD2, isolated from *G. cowa* Roxb. ex Choisy (Asam kandis) leaves, revealed Aurasperone B and Fonsecinone B as the dominant bioactive metabolites. The ethyl acetate extract exhibited notable cytotoxicity against *A. salina* larvae (LC_{50} = 79.45 µg/mL) and potent inhibition of MCF-7 breast cancer cells (IC_{50} = 14.45 µg/mL). Molecular docking suggested strong binding affinities of these compounds to MRSA and breast cancer-related receptors, supporting their potential as antibacterial and anticancer agents. However, these

findings are limited to *in vitro* assays and computational predictions; the mechanisms of action remain to be fully elucidated. *In vivo* validation, toxicity profiling, and pharmacokinetic studies are crucial for assessing the therapeutic potential and safety of these compounds. Future work should focus on isolating and purifying these active compounds, confirming their bioactivities in animal models, and exploring the structure–activity relationships to optimize efficacy. Such efforts will be crucial to advancing *A. terreus* GCD2-derived metabolites toward pharmaceutical applications.

Ethics approval

This research protocol was evaluated by the Research Ethics Committee of the Faculty of Medicine, Andalas University, and received a positive assessment following a review of the study design, research protocol, and use of experimental animals. The ethical approval number is 133/UN.16.2/KEP-FK/2024.

Acknowledgements

This research was supported by the BOPTN Universitas Andalas, Riset Publikasi Terindeks (RPT) program, Indonesia, under contract number T/10/UN16.19/PT.01.03/KO-RPT/2023.

Declaration of Generative AI in Scientific Writing

The authors acknowledge the use of generative AI tools (e.g., QuillBot, Grammarly, and ChatGPT by OpenAI) in the preparation of this manuscript, specifically for language editing and grammar correction. No content generation or data interpretation was performed by AI. The authors take full responsibility for the content and conclusions of this work.

CRediT Author Statement

Muhammad Azhari Herli: Methodology; Investigation; Data curation; validation; Writing - Original draft; Visualization. **Putri Ulinza**: Investigation; Data curation; Validation. **Netti Suharti**: Supervision; Writing - Reviewing and Editing. **Djong Hong Tjong**: Supervision; Writing - Reviewing and Editing. **Dian Handayani**: Conceptualization; supervision; Methodology; Preparation; Data curation; validation; Writing - Reviewing and Editing.

References

[1] K Panthong, W Pongcharoen, S Phongpaichit and WC Taylor. Tetraoxygenated xanthones from the fruits of *Garcinia cowa. Phytochemistry* 2006; **67(10)**, 999-1004.

[2] T Ritthiwigrom, S Laphookhieo and SG Pyne. Chemical constituents and biological activities of *Garcinia cowa* Roxb. *Maejo International Journal of Science and Technology* 2013; **7(2)**, 212-231.

[3] K Panthong, N Hutadilok-Towatana and A Panthong. A new tetraoxygenated xanthone, and other anti-inflammatory and antioxidant compounds from *Garcinia cowa*. *Canadian Journal of Chemistry* 2009; **87(11)**, 1636-1640.

[4] A Sarma, P Sarmah, D Kashyap and A Kalita. Evaluation of nutraceutical properties and antioxidant activity of *Garcinia cowa* Roxb. ex Choisy fruits found in Assam (India). *World Journal of Pharmacy and Pharmaceutical Sciences* 2014; **3(12)**, 553-559.

[5] A Chouni and S Paul. A comprehensive review of the phytochemical and pharmacological potential of an evergreen plant, *Garcinia cowa*. *Chemistry & Biodiversity* 2023; **20(2)**, e202200910.

[6] NTK An, NV Hien, NT Thuy, DL Phuong, HG Bach, NT Tra, NQ Tung, PT Tham, BH Tai and TTT Thuy. Garcicowanones C-E, three new hydrated-geranylated xanthones from the roots of *Garcinia cowa* Roxb. ex Choisy, and their α-glucosidase inhibition activities. *Natural Product Research* 2023; **37(21)**, 3668-3676.

[7] HL Devi, B Das, T Angami and B Kandpal. *Garcinia cowa* Roxb. ex Choisy (Clusiaceae). *In:* AA Waman and P Bohra (Eds.). Perennial underutilized horticultural species of India. Jaya Publishing House, Delhi, India, 2021, p. 131-143.

[8] F Eshboev and D Egamberdieva. *Medicinal plant-associated endophytic fungi: Metabolites and bioactivity*. *In:* D Egamberdieva, JA Parray and K Davranov (Eds.). Plant endophytes and secondary metabolites. Academic Press, Cambridge, UK, 2024, p. 95-104.

[9] A Yang, Y Hong, F Zhou, L Zhang, Y Zhu, C Wang, Y Hu, L Yu, L Chen and X Wang. Endophytic microbes from medicinal plants in Fenghuang mountain as a source of antibiotics. *Molecules* 2023; **28(17)**, 6301.

[10] D Handayani, RI Muslim, N Syafni, MA Artasasta and R Riga. Endophytic fungi from medicinal plant *Garcinia cowa* Roxb. ex Choisy and their antibacterial activity. *Journal of Applied Pharmaceutical Science* 2024; **14(9)**, 182-188.

[11] N Sandrawati, SP Hati, F Yunita, AE Putra, F Ismed, TE Tallei, T Hertiani and D Handayani. Antimicrobial and cytotoxic activities of marine sponge-derived fungal extracts isolated from *Dactylospongia* sp. *Journal of Applied Pharmaceutical Science* 2020; **10(4)**, 028-033.

[12] J Mani, J Johnson, H Hosking, BE Hoyos, KB Walsh, P Neilsen and M Naiker. Bioassay-guided fractionation protocol for determining novel active compounds in selected Australian flora. *Plants* 2022; **11(21)**, 2886.

[13] B Meyer, N Ferrigni, J Putnam, L Jacobsen, D Nichols and J McLaughlin. Brine shrimp: A convenient general bioassay for active plant constituents. *Planta Medica* 1982; **45(5)**, 31-34.

[14] P Kumar, A Nagarajan and PD Uchil. Analysis of cell viability by the MTT assay. *Cold Spring Harbor Protocols* 2018; **2018(6)**, 469-471.

[15] JV Meerloo, GJL Kaspers and J Cloos. *Cell sensitivity assays: The MTT assay. In:* IA Cree (Ed.). Cancer cell culture. Humana press, New Jersey, USA, 2011, p. 237-245.

[16] D Handayani, W Rasyid, EN Zainudin and T Hertiani. Cytotoxic activity screening of fungal extracts derived from the West Sumatran marine sponge *Haliclona fascigera* to several human cell lines: HeLa, WiDr, T47D, and Vero. *Journal of Applied Pharmaceutical Science* 2018; **8**, 055-058.

[17] GS Guide, MassLynx 4.1, Available at: http://argenta2.chem.unr.edu/downloads/LCMS%20Waters %20MassLynx4.1%20 Manual.pdf, accessed January 2025.

[18] W Zhang, X Li, X Ji and M Gouda. *Use of LC-Q-TOF-MS for elucidating the flavonoids. In:* M Gouda, X Li and Y He (Eds.). Plant chemical compositions and bioactivities. Humana Press, New York, 2024, p. 165-191.

[19] W Li, J Zhang and LS Francis. *Handbook of LC-MS bioanalysis: Best practices, experimental protocols, and regulations.* Wiley, New Jersey, USA, 2013, p. 704.

[20] B Zhou, JF Xiao, L Tuli and HW Ressom. LC-MS-based metabolomics. *Molecular BioSystems* 2012; **8(2)**, 470-481.

[21] TE Tallei and BJ Kolondam. DNA barcoding of Sangihe Nutmeg (*Myristica fragrans*) using matK gene. *HAYATI Journal of Biosciences* 2015; **22(1)**, 41-47.

[22] K Tamura, G Stecher and S Kumar. MEGA11: Molecular evolutionary genetics analysis version 11. *Molecular Biology and Evolution* 2021; **38(7)**, 3022-3027.

[23] RW Birkinshaw, J Gong, CS Luo, D Lio, CA White, MA Anderson, P Blombery, G Lessene, IJ Majewski, R Thijssen, AW Roberts, DCS Huang, PM Colman and PE Czabotar. Structures of BCL-2 in complex with venetoclax reveal the molecular basis of resistance mutations. *Nature Communications* 2019; **10(1)**, 2385.

[24] RCSB PDB - 6O0K, Crystal structure of BCL-2 with venetoclax, Available at: https://www.rcsb.org/structure/6O0K, accessed June 2025.

[25] RCSB PDB - 6Q9N, Crystal structure of PBP2a from MRSA in complex with piperacillin and quinazolinone, Available at: https://www.rcsb.org/structure/6Q9N, accessed June 2025.

[26] J Janardhanan, R Bouley, S Martínez-Caballero, Z Peng, M Batuecas-Mordillo, JE Meisel, D Ding, VA Schroeder, WR Wolter, KV Mahasenan, JA Hermoso, S Mobashery and M Chang. The quinazolinone allosteric inhibitor of PBP 2a synergizes with piperacillin and tazobactam against methicillin-resistant *staphylococcus aureus*. *Antimicrobial Agents and Chemotherapy* 2019; **63(5)**, e02637.

[27] MC Nagtilak. *Molecular docking: A highly efficient method for structure-based drug designing. In:* VA Chavan, PS Sagar, R Shukla, E Laxminarayana, A Debnath, S Supriya, U Das and S Vijayakumar (Eds.). Futuristic trends in chemical material sciences & nano technology. Iterative International Publishers, Michigan, USA, 2024, p. 97-106.

[28] Molecular Docking With Molecular Operating Environment (MOE), Available at: https://www.chemcomp.com/

moe/help/latest/index_tut.html, accessed November 2024.

[29] BD Systèmes. *Discovery Studio Visualizer Software.* Accelrys, San Diego, 2021.

[30] E Udayan and JJ Gnanadoss. Potential of endophytic fungi as therapeutics: Antibiotics, antiviral and anticancer properties. *Research Journal of Biotechnology* 2023; **18(6)**, 132-145.

[31] SK Deshmukh, L Dufossé, H Chhipa, S Saxena, GB Mahajan and MK Gupta. Fungal endophytes: A Potential source of antibacterial compounds. *Journal of Fungi* 2022; **8(2)**, 164.

[32] SJ Li, X Zhang, XH Wang and CQ Zhao. Novel natural compounds from endophytic fungi with anticancer activity. *European Journal of Medicinal Chemistry* 2018; **156**, 316-343.

[33] D Handayani, MA Artasasta, D Mutia, N Atikah, Rustini and TE Tallei. Antimicrobial and cytotoxic activities screening of fungal secondary metabolites isolated from marine sponge *Callyspongia* sp. *AACL Bioflux* 2021; **14(1)**, 249-258.

[34] MA Artasasta, Y Yanwirasti, M Taher, A Djamaan, NP Ariantari, RA Edrada-Ebel and D Handayani. Apoptotic activity of new oxisterigmatocystin derivatives from the marine-derived fungus *Aspergillus nomius* NC_{06}. *Marine Drugs* 2021; **19(11)**, 631.

[35] Aspergillus terreus, Doctor Fungus, Available at: https://drfungus.org/knowledge-base/aspergillus-terreus/, accessed June 2025.

[36] C Lass-Flörl, AM Dietl, DP Kontoyiannis and M Brock. *Aspergillus terreus* species complex. *Clinical Microbiology Reviews* 2021; **34(4)**, e0031120.

[37] P Kapli, Z Yang and MJ Telford. Phylogenetic tree building in the genomic age. *Nature Reviews Genetics* 2020; **21(7)**, 428-444.

[38] MS Lestari, T Himawan, AL Abadi and R Retnowati. Toxicity and phytochemistry test of methanol extract of several plants from papua using *Brine Shrimp Lethality Test* (BSLT). *Journal of Chemical and Pharmaceutical Research* 2015; **7(4)**, 866-872.

[39] H Niksic, F Becic, E Koric, I Gusic, E Omeragic, S Muratovic, B Miladinovic and K Duric. Cytotoxicity screening of *Thymus vulgaris* L. essential oil in brine shrimp nauplii and cancer cell lines. *Scientific Reports* 2021; **11(1)**, 13178.

[40] S Ghosal, K Biswas and DK Chakrabarti. Toxic naphtho-.gamma.-pyrones from Aspergillus niger, *Journal of Agricultural and Food Chemistry* 1979; **27(6)**, 1347-1351.

[41] S Padhi, M Masi, SK Panda, W Luyten, A Cimmino, K Tayung and A Evidente. Evidente, antimicrobial secondary metabolites of an endolichenic Aspergillus niger isolated from lichen thallus of Parmotrema ravum. *Natural Product Research* 2020; **34(18)**, 2573-2580.

[42] Dulcioic acid | C7H12O8, Available at: https://www.chemspider.com/Chemical-Structure.29365152.html, accessed July 2025.

[43] 8-Benzyl-3-(4-biphenylyl)-4,9-dimethyl-7H-furo[2,3-f]chromen-7-one,$C_{32}H_{24}O_3$, https://www.chemspider.com/Chemical-Structure.1385615.html, accessed July 2025.

[44] PubChem, Malformin A, Available at: https://pubchem.ncbi.nlm.nih.gov/compound/4005, accessed June 2025.

[45] PubChem, Aurasperone B, Available at: https://pubchem.ncbi.nlm.nih.gov/compound/179522, accessed June 2025).

[46] PubChem, Fonsecinone B, Available at: https://pubchem.ncbi.nlm.nih.gov/compound/101301306, accessed June 2025.

[47] Aurasperone A, $C_{32}H_{26}O_{10}$, Available at: https://www.chemspider.com/Chemical-Structure.2341316.html, accessed July 2025.

[48] K Palaniveloo, KH Ong, H Satriawan, SA Razak, S Suciati, HY Hung, S Hirayama, M Rizman-Idid, JK Tan, YS Yong and SM Phang. *In vitro* and *in silico* cholinesterase inhibitory potential of metabolites from Laurencia snackeyi (Weber-van Bosse) M. Masuda. 3 Biotech 2023; **13(10)**, 337.

[49] SA Attique, M Hassan, M Usman, RM Atif, S Mahboob, KA Al-Ghanim, M Bilal and MZ Nawaz. A molecular d ocking approach to evaluate the pharmacological properties of natural and synthetic treatment candidates for use against hypertension. *International Journal of Environmental Research and Public Health* 2019; **16(6)**, 923.

[50] H Purnomo. *Kimia Komputasi: Molecular docking plants-penambatan molekul plants (protein ligand ant system).* Pustaka Pelajar, Yogyakarta, 2011.

[51] S Mukherjee, TE Balius and RC Rizzo. Docking validation resources: Protein family and ligand flexibility experiments. *Journal of Chemical Information and Modeling* 2010; **50(11)**, 1986-2000.